



Deficiency of Healthcare Accessibility of Elderly People Exposed to Future Extreme Coastal Floods: A Case Study of Shanghai, China

Xinmeng Shan^{1,2,3,4} · Paolo Scussolini⁴ · Jun Wang^{1,2,3} · Mengya Li⁵ · Jiahong Wen⁶ · Lei Wang⁷

Accepted: 30 September 2023 / Published online: 31 October 2023
© The Author(s) 2023

Abstract

Socioeconomic development, subsidence, and climate change have led to high flood risks in coastal cities, making the vulnerable, especially elderly people, more prone to floods. However, we mostly do not know how the accessibility of life-saving public resources for the elderly population will change under future scenarios. Using Shanghai as a case, this study introduced a new analytical framework to fill this gap. We integrated for the first time models of coastal flooding, local population growth, and medical resource supply-demand estimation. The results show that under an extreme scenario of coastal flooding in the year 2050, in the absence of adaptation, half of the elderly population may be exposed to floods, the supply of medical resources will be seriously insufficient compared to the demand, and the accessibility of emergency medical services will be impaired by flooding. Our methodology can be applied to gain insights for other vulnerable coastal cities, to assist robust decision making about emergency responses to flood risks for elderly populations in an uncertain future.

Keywords Coastal floods · Elderly population · Flood exposure analysis · Healthcare accessibility · Shanghai

1 Introduction

Flooding in coastal zones is one of the most devastating natural hazards, accounting for approximately one-third of all global disaster losses and over half of total casualties

(Wolff et al. 2020; Tellman et al. 2021). In 2012 Hurricane Sandy, for example, caused the most destructive flooding over New York City by generating the highest storm tide in the city's history, resulting in considerable casualties (45 deaths), damages, and extensive indirect impacts (for example, the city's infrastructure and public services were disrupted) (NYC OEM 2014). Hurricane Katrina in 2005 had a devastating impact on residents of the Gulf Coast, killing at least 1833 people (Gallagher and Hartley 2017). In the context of climate change, sea level rise, land subsidence, and rapid urban growth, flood risk in coastal cities may increase significantly (Fang et al. 2021; Fang et al. 2022). According to the research by Kirezci et al. (2020), under the RCP8.5 emission scenario¹ (Hausfather and Peters 2020), 176–287 million people may suffer from coastal floods in 2100, and the total assets exposed could reach up to USD 14,178 billion, accounting for 20% of global GDP. Many coastal cities, especially Shanghai in Asia, are highly populated and will face increasing flood risks due to future sea level rise and socioeconomic development (Liang et al. 2017; Cheng 2020; Du et al. 2020). Vulnerable groups such as the elderly, children, and people with poor health are disproportionately affected by floods (Yu et al. 2020). Therefore, special

✉ Paolo Scussolini
p.scussolini@vu.nl

✉ Jun Wang
jwang@geo.ecnu.edu.cn

¹ Key Laboratory of Geographic Information Science (Ministry of Education), East China Normal University, Shanghai 200241, China

² Institute for National Safety and Emergency Management, East China Normal University, Shanghai 200062, China

³ School of Geographic Sciences, East China Normal University, Shanghai 200241, China

⁴ Institute for Environmental Studies, Vrije Universiteit Amsterdam, 1081 HV Amsterdam, The Netherlands

⁵ School of Public Management, East China Normal University, Shanghai 200062, China

⁶ School of Environmental and Geographical Sciences, Shanghai Normal University, Shanghai 200234, China

⁷ Department of Geography & Anthropology, Louisiana State University, Baton Rouge, LA 70803, USA

¹ The RCP8.5 scenario refers to the highest greenhouse gas emissions and is a worst-case scenario.

attention needs to be addressed to open questions about how to estimate the exposure and vulnerability of vulnerable populations during floods. This is important to accurately inform decision makers and the public about the public safety consequences of higher flood risks.

Risk is a function of hazard, exposure, and vulnerability (Kron 2005). In the context of flood risk to people, exposure is used to indicate the population situated in the area of the potential flood hazard. Vulnerability here indicates the extent to which people are negatively affected by the occurrence of the hazard. A main determinant of vulnerability of people is their age. Several studies have found that the elderly populations in flooded areas are more negatively impacted. The elderly often have limited mobility, greater healthcare access needs, and therefore significantly higher mortality rates during disasters (Bukvic et al. 2018; Lome-Hurtado et al. 2021; Sawangnate et al. 2022). For these reasons, flooding from Hurricane Katrina caused a disproportionately high death rate among the elderly population, with 64% of deaths occurring in the population over the age of 65 (Zoraster 2010). Almost half of the casualties from Hurricane Sandy were also over the age of 65 (Kan and Lejano 2023). Liang et al. (2017) analyzed population exposure in rainstorm hazard areas in China and found that, from 1990 to 2010, the population exposed increased by 110 million, corresponding to 14.6%, indicating that the total exposed population in 2030 will be 1,000 million, and the exposed elderly population will reach 139 million.

This phenomenon is all the more cogent given the worldwide aging of populations caused by low birth rates and growing life spans (Gill et al. 2012; Wang and Yarnal 2012; Chien and Chen 2017; Bai and Lei 2020), especially in China, where the total fertility rate fell sharply between 1960 and 2017 from 5.8 to 2.3, below the sustainable level. By 2049, China's population over the age of 65 is projected to reach 399 million, accounting for more than a quarter (29%) of the total population. What should be done with increased future exposure and risks for the elderly population, under scenarios of climate change and demographic development, in order to rationally plan future medical and emergency services? To answer this question, we need to gain knowledge about future flood extent, demographics of exposure, and medical and emergency resource supply-demand ratios, using rigorous analytical models.

Centralized service providers, such as emergency medical services or emergency response services, play a crucial role in rescue and relief efforts during natural hazard and disaster events (Coles et al. 2017; Liu et al. 2019; Li et al. 2021). The effectiveness of these services is often evaluated in terms of accessibility (Coles et al. 2017; Yang and Mao 2018; Rizeei et al. 2019; Xia et al. 2019; Kiran et al. 2020; Yang et al. 2020; Yu et al. 2020). The reduced average mobility of the elderly population is an accessibility disadvantage

(Crimmins 2016) that is amplified by the interruption of transportation and the demise of emergency response centers during flooding (Yin, Yu, et al. 2020). Coles et al. (2017) assessed the accessibility of emergency services during two flood events in the city of York, U.K., by combining a hydrodynamic model with a geographic analysis of accessibility. Another case study in the city of Leicester, U.K. by Green et al. (2017) studied the accessibility of ambulance and fire and rescue services during floods with different return periods.

However, explicit analysis of the flood emergency situation of the elderly population is rare, and does not include analysis of the supply-demand ratio of medical resources for the elderly. Furthermore, there is rare consideration of low-likelihood, high-magnitude floods, and of future developments. For this reason, we developed a multidisciplinary analysis framework that consists of a coastal flood model, a population growth model, and a medical resource supply-demand and emergency medical center accessibility analysis model. We then applied the framework to the city of Shanghai. We addressed two questions:

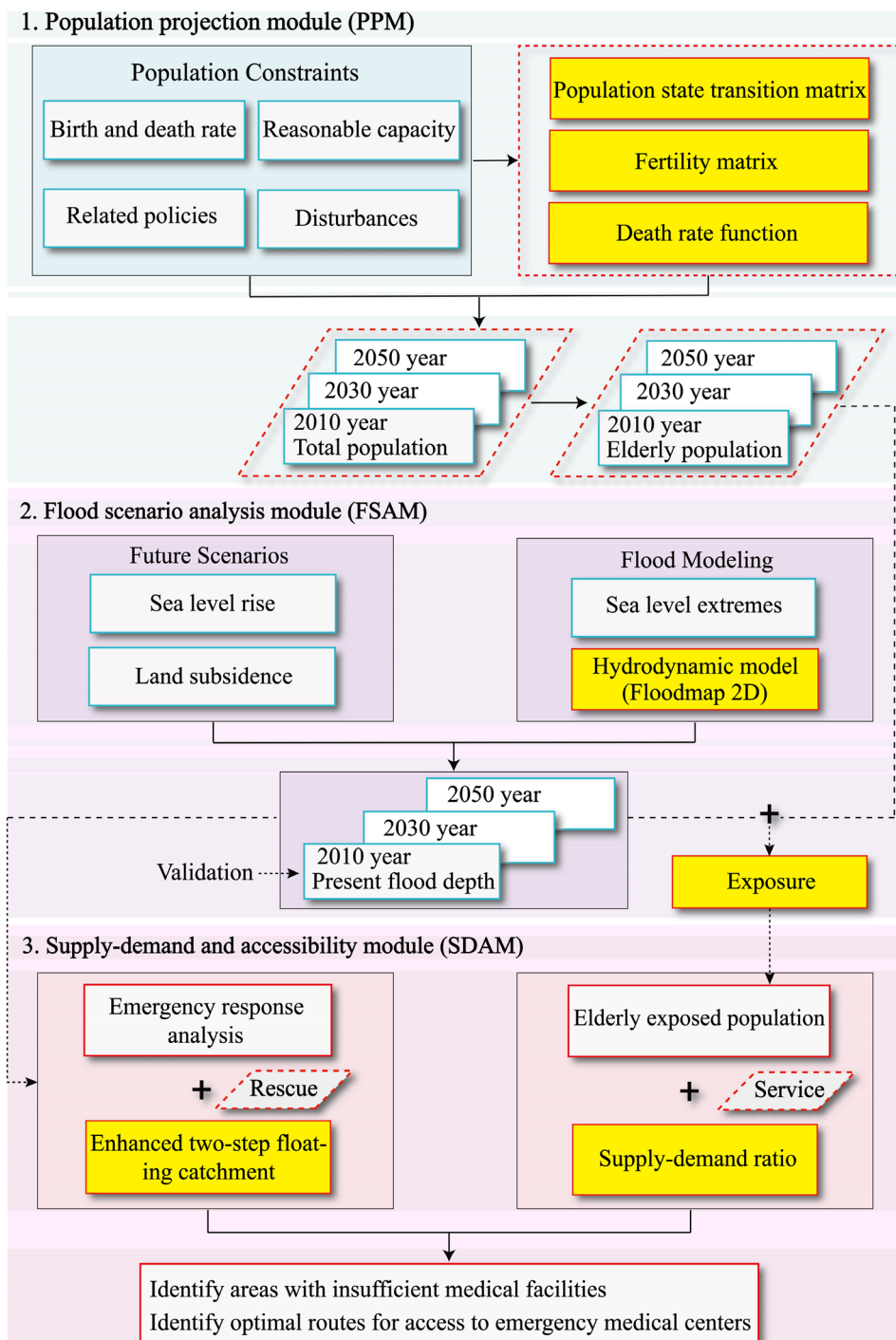
- (1) How will the supply-demand ratio of medical services change in the future, due to sea level rise and changes in demographics? and
- (2) How will the elderly's accessibility to emergency medical centers during coastal floods change in the future, and when a flood occurs, can the number of medical services meet the needs of rescuing the elderly in the future?

The framework is easily generalizable to other cities, and we provide guidelines on the datasets necessary for the scope of such an analysis. This in turn can provide the scientific basis for policies aimed at reducing the flood vulnerability of the elderly.

2 Methods

We integrated three analysis modules: (1) a population projection module (PPM); (2) a flood scenario analysis module (FSAM); and (3) a supply-demand and accessibility module (SDAM) (Fig. 1). The total population was projected by the PPM for the years 2030 and 2050, using historical and current population census data as input. To project the spatial distribution of the elderly population, we combined the changes of the elderly population in Shanghai in the past 30 years with the proportion of the elderly population in each administrative unit. The FSAM models flood inundation maps for 2030 and 2050, with consideration of different scenarios of climate and sea level rise, and land subsidence. The SDAM evaluates

Fig. 1 The methodology framework of the healthcare accessibility study in Shanghai



the supply-demand ratio of medical resources and the accessibility of emergency medical centers for the elderly population, by superimposing the new flood maps, the new population projection maps, and existing maps of transportation infrastructure and medical services.

2.1 Population Projection Module (PPM)

Coastal cities are densely populated, and future population projections based on coarse spatial resolution analysis may cause significant bias in extreme flood risk analysis (Tang

et al. 2021). In this step, we refined future projections of population. We adopted the method of Qiu et al. (2014) and Song et al. (1981), which considers birth and death rates, constraints such as the capacity of a place to accommodate the population and population-related governmental policies, and migration, as shown in the following equations. At any given moment in time, the population of a defined age is calculated as:

$$x_i(t) = \int_i^{i+1} p(r, t) dr, i = 0, 1, 2, \dots, m, \tag{1}$$

where $x_i(t)$ represents the number of people in the age interval $[i, i+1]$ in year t , while $p(r, t)$ represents the population age density function, r represents age, and i is an integer with a value from 0 to m , with m representing maximum life span. The population state vector $x(t)$, representing the population age composition, is:

$$x(t) = \{x_0(t), x_1(t), \dots, x_m(t)\}, \tag{2}$$

$$y(t) = \beta(t) \sum_{i=r_1}^{r_2} k_i(t) h_i(t) x_i(t), \tag{3}$$

where $y(t)$ is the absolute birth rate, $\beta(t)$ is the average fertility rate of women, $k_i(t)$ is the sex ratio function, $k_i(t)x_i(t)$ is the total number of women aged i in the t generation, $h_i(t)$ is the reproductive pattern of women, and $\beta(t) h_i(t)$ represents the average number of babies born to a woman aged i in 1 year from $t-1$ to t . Therefore, $\beta(t) h_i(t) k_i(t) x_i(t)$ is the number of babies born to all women whose age is i in the t generation. When i changes from r_1 to r_2 , adding them up is the number of babies born to all women in the childbearing age interval $[r_1, r_2]$ in the t generation, that is, $y(t)$.

Not all of these babies survived to the statistical moment of the t generation, and some of them died due to diseases and other reasons. The number of babies who survive to the statistical moment of the t generation is $x_0(t)$, calculated by Eq. 4. Accordingly, $y(t) - x_0(t)$ is the number of babies who do not survive from $t-1$ to the t generation, defined as the baby mortality rate $\mu_{00}(t)$, calculated by Eq. 5:

$$x_0(t) = (1 - \mu_{00}(t))y(t). \tag{4}$$

$$\mu_{00}(t) = \frac{y(t) - x_0(t)}{y(t)}. \tag{5}$$

Then, we introduced vector and matrix notation, $i = r_1, r_1+1, \dots, r_2$, expressed as Eq. 6:

$$b_i(t) = (1 - \mu_{00}(t))(1 - \mu_0(t))k_i(t)h_i(t), \tag{6}$$

$$H(t) = \begin{bmatrix} 0 & 0 & 0 & \dots & 0 \\ 1 - \mu_1(t) & 0 & 0 & \dots & 0 \\ 0 & 1 - \mu_2(t) & 0 & & 0 \\ & & \vdots & & \vdots \\ 0 & 0 & & 1 - \mu_{m-1}(t) & 0 \end{bmatrix}, \tag{7}$$

$$f(t) = \{f_1(t), f_2(t), f_3(t), \dots, f_m(t)\}, \tag{8}$$

where $H(t)$ is the population state transition matrix from t to $t+1$, $B(t)$ is the fertility matrix, $\mu(t)$ is a function of the mortality rate, $f(t)$ is the population migration vector, and b is a constant. Equation 9 is thus written in vector form:

$$\begin{cases} x(t+1) = H(t)x(t) + \beta(t)B(t)x(t) + f(t), \\ x(0) = \{x_1(0), x_2(0), x_3(0), \dots, x_m(0)\} \\ \sum_{a=x_0(t)}^{x_i(t)} x(a) \leq b \end{cases} \tag{9}$$

where b is the total population in year t . The possible future population capacity can be determined according to urban development planning and previous research. In this study, we considered two factors:

- (1) The population forecast for Shanghai in 2035. Shanghai’s urban master plan (2017–2035) proposes that the resident population will be limited to around 25 million; and
- (2) The historical trend of Asian population agglomeration areas such as Tokyo (Wang 2003) and the research of Wang et al. (2014) predicts that in 2050, considering migration factors, the total population of Shanghai will be about 34.3 million. Therefore, we assumed that the total population of Shanghai will not exceed 35 million before 2050.

The PPM cannot predict the change of the elderly population, so we used an additional method for this. A polynomial curve was fitted on 30 years of data on the number of Shanghai’s elderly population, published by the Shanghai Statistical Yearbook (1990–2020), which was then extrapolated to obtain the total elderly population in the future. The spatial distribution of the future elderly population was obtained by assuming that the proportion of the elderly population in each administrative unit remains stable.

2.2 Flood Scenario Analysis Module (FSAM)

The FloodMap-Inertial 2D model (Yu and Coulthard 2015) was used to construct a 50 m high-resolution coastal flood simulation model. The hazards include sea level rise, the impact of extreme water levels caused by storm surges, and riverine floods. The flood modeling and estimation

was based on a reliability analysis, using the actual seawall and floodwall heights to calculate the compound effect of overflow and dike breach to derive dike failure. Hydrostatic hydrographs recorded along the coast and along the Huangpu River and boundary measurement stations were used to generate dynamic boundary conditions for the flood model (that is, time series of water levels) for 10-year, 100-year, and 1,000-year flood return periods (Yin, Jonkman, et al. 2020), which is done by scaling the stage hydrographs recorded by boundary gauge stations during 1997 Typhoon Winnie (historically worst case). Relative sea level rise was estimated by combining the climate-driven absolute sea level rise predicted by the Lvsi station in the Yangtze River Delta with a linear approximation of the future subsidence rate (6 ± 1 mm/year) in Shanghai (Yin et al. 2013). The relative sea level projections for 2100 were all based on 2010. The local or relative sea level rise projections for Shanghai were based on the research by Yin, Jonkman, et al. (2020). The city-scale and street-level modeling framework has been verified in multiple cases, including New York (Yin et al. 2016) and Shanghai (Yin, Jonkman, et al. 2020), and can perform high-level prediction of inland flooding.

2.3 Supply-Demand and Accessibility Module (SDAM)

We used three categories of points of interest (POIs). The supply-demand ratio was evaluated for the first and second types of medical facilities, and the accessibility analysis was performed for the third type of emergency medical centers.

The supply of a certain type of medical service denotes the number of the corresponding medical facilities weighted by a distinctive capacity. Two categories of medical facilities were considered: (1) pharmacies, health products stores, clinics, and centers for disease control; and (2) general hospitals and specialist hospitals. Each type of medical facilities (for example, pharmacies) were counted by their POIs. The supply to demand ratio in a neighborhood committee² (NC) during a flood is computed by Eq. 10:

$$SDR_i = \frac{S_{1i} \times W_1 + S_{2i} \times W_2}{P_{ield}}, \tag{10}$$

where SDR_i represents the supply-demand ratio of NC_i , P_{ield} is the projected elderly population in NC_i , S_{1i} is the number of medical facilities of the first category (that is, pharmacies, health products stores, clinics, and centers for disease control), while S_{2i} is the number of medical facilities of the second category (that is, general hospitals and specialist hospitals). W_j ($j = 1, 2$) is the average capacity of facilities in

the j -th category, which is calculated as $W_j = P_b/S_j$, where P_b and S_j , respectively, denote the total population and the total number of medical facilities belonging to the j -th category in the entire study area.

Note that P_b is the population in 2010. China has conducted a national census every 10 years since 1990. The latest official census data from 2020, that is, those of the Seventh Census, were released in 2021, but some data are not accessible to the public and researchers yet. Lacking the latest subdistrict/township-level population data in Shanghai, we used the Sixth Census data (that is, population in 2010) as an alternative. We assumed that W_1 and W_2 remain the same as 2010 in the future scenarios. Additionally, a facility located in a flooded area with water depth over 0.35 m will be considered not operational and excluded from facilities counted for estimating service supply (Yin et al. 2011).

For elderly people, also critical during floods are the emergency medical centers, which provide essential life-saving services during disasters, such as medical stabilization on site and transportation to hospitals. When flood water depth in Shanghai exceeds 30 cm—a general threshold for road closures in many cities of the world (Arrighi et al. 2019; Yin, Yu, et al. 2020; Yu et al. 2020)—emergency medical centers cannot be accessed. Affected roads in NCs were first identified by overlapping roads with defined flood areas, but viaducts and bridges were excluded. A schematic diagram of the spatial accessibility of the emergency medical centers is shown in Fig. 2.

We set the average intervention radius of emergency medical centers to 4 km (Li et al. 2022). Therefore, the emergency accessibility analysis was performed only for destinations within a 4 km radius of the emergency medical centers. We used the generalized two-step floating catchment area (G2SFCA) method to measure emergency medical center accessibility (Li et al. 2022). The distance decay behavior was described by a continuous function (Wang 2015). We did not consider constraints from urban road traffic rules such as traffic lights. Route distance was used in the G2SFCA algorithm to calculate the accessibility in NC_i . The level of accessibility, A_i , was calculated according to Eq. 11:

$$A_i = \sum_{k=1}^n \left(\frac{S_k f_{d(i,k)}}{\sum_{j=1}^m P_j f_{d(j,k)}} \right), \tag{11}$$

where S_k is the capacity of emergency medical center k . We used ambulance and rescue vehicles to characterize emergency center’s capabilities. We cannot estimate how supply may vary from center to center. Thus, all S_k capacity was assumed to be 1 (unit). P_j is the population of NC_j , n is the demand point, defined here as the centroid of the NC polygon. m is the number of demand locations that are

² Neighborhood committees are the smallest administrative units of the census data in urban areas of China (Gu et al. 2018).

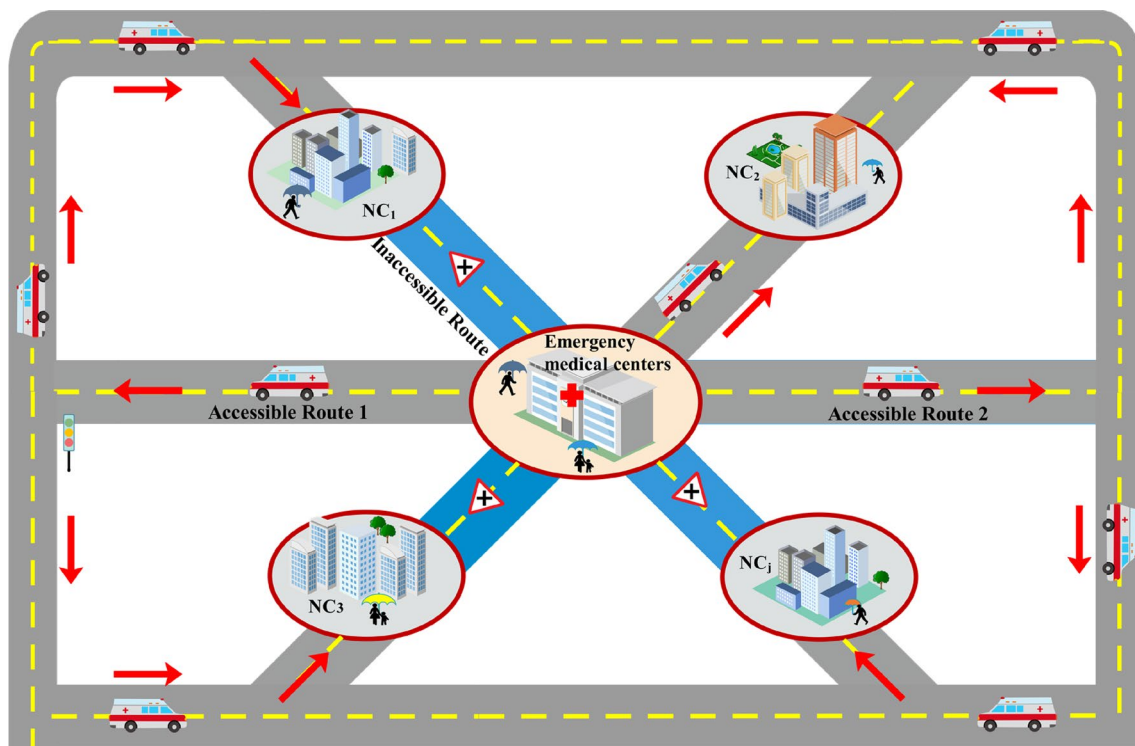


Fig. 2 Schematic diagram of the spatial accessibility of emergency medical centers in Shanghai. Note: In the blue area water depth exceeds 30 cm. *NC* neighborhood committee, *NC_j* represents the *j*-th neighborhood committee.

accessible in NC_j within a threshold distance, d_0 . $f_{d(ik)}$ is the travel impedance, which is determined by road connectivity and affected by road closures caused by extreme floods. With road closures, the shortest distance routes will be researched through the network until another route is found, or the route will be marked as “non-available” if no solution can be found. The $f_{d(ik)}$ takes the form of a modified Gaussian function $e^{-d(ik)/2\alpha}$, where $d(ik)$ is the shortest route distance between station k (S_k) and NC_j , and the parameter α determines the function’s rate of decline and the point where it approaches zero. $f_{d(ik)}$ has the same meaning as $f_{d(jk)}$. We assumed that $f_{d(ik)}$ equals 0 when $d(ik)$ equals d_0 , based on which α was computed. Here, we assumed that d_0 equals 4 km. That is, the emergency access routes with a Euclidian distance over 4 km were initially removed from the routing calculation, and more than 30,000 routes are available in the transportation network (see Sect. 3.3 for detailed data sources).

3 Study Area and Data Processing

Shanghai, the largest port city in the world, located at the mouth of the Yangtze River, had an area of 6,340 km² and 24.88 million residents as of 2020. The city is built on a low-lying coastal plain tilting from east to west with an average

elevation of about 4 m. The eastern tip and the northeastern and southeastern parts of the area stretch into the East China Sea, with the Huangpu River and the Suzhou River running through the center (Fig. 3).

Shanghai is heavily prone to compound impacts of storm surges, high astronomic tides, heavy rains, and fluvial floods (Wang et al. 2012; Wang et al. 2018). According to the statistics, Shanghai is hit by typhoon storms twice a year on average, up to 6 to 7 times a year (Chen and Wang 2000). Severe typhoon storms occurred, for example, during Typhoon Winnie in 1997, Typhoon Matsa in 2005, Typhoon Fitow in 2013, Typhoon Lekima in 2019, and Typhoon In-fa in 2021. One of the deadliest storm surge events killed more than 29,000 people in Shanghai in 1905; Typhoon Winnie killed seven people and flooded more than 5000 residences in 1997. During typhoon Winnie, Shanghai suffered the first so-called “four encounters” disaster of wind, storm, tide, and flood since 1949. The tidal levels along the Yangtze River Estuary and the Huangpu River exceeded historical records, and the resulting floods overflowed the urban flood control walls in nearly 20 places and breached the walls in three places. Considering the superimposed effects of sea level rise, land subsidence, and socioeconomic development, the risk of Shanghai suffering from compound extreme flood disasters may further increase in the future (Xian et al. 2018).

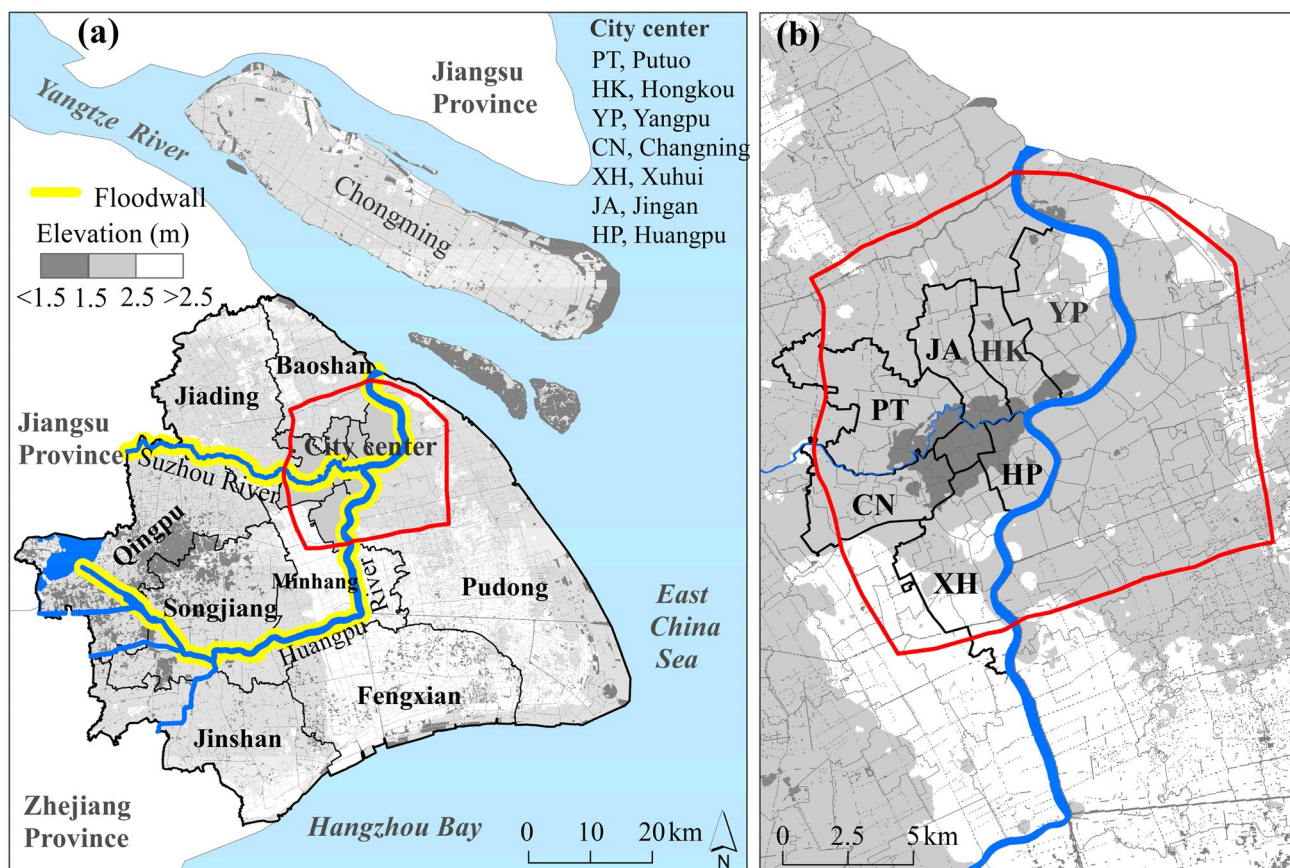


Fig. 3 Shanghai's location and elevation (a) and the city center (b)

3.1 Population Data

Population data include total population and elderly population. Administrative units in Shanghai are divided into the hierarchical levels of districts, subdistricts/townships, and neighborhood committees (NCs). In our study area, there are 5432 NCs that function as demand locations. The total population distribution in 1990–2010 was disaggregated from Shanghai subdistrict/township-level census data—derived from the fourth, fifth, and sixth population censuses of China—which cover more than 100 factors such as age, fertility, mortality, life expectancy, and sex ratio at birth. People over the age of 65 are considered the elderly population.

3.2 Flood Modeling Data

Data input for flood modeling for this study included: (1) Digital elevation data constructed from 0.5-m interval contour lines, with a resolution of 50 m and a vertical accuracy of 0.1–0.2 m, and a higher-resolution (5 m) digital elevation dataset for the financial center (Yin, Jonkman, et al. 2020); (2) Station-based tide levels of Shanghai Water Authority in the last decade (Yin, Jonkman, et al. 2020); (3) The localized

sea level rise projections at Lvsi gauge station located in the Yangtze River Delta, under the RCP2.6³ (Hausfather and Peters 2020) and RCP8.5 emission scenarios (Kopp et al. 2014); (4) Land subsidence data of the whole city since 2000 (Yin, Jonkman, et al. 2020); and (5) Floodplain topography (Yin, Jonkman, et al. 2020).

3.3 Point of Interest (POI) and Transportation Network Data

Data of POIs in 2020 were extracted through a web crawling program from Amap.⁴ The POIs were classified into three categories based on the type of services (Fig. 4a, b, c), which include the first category of pharmacies, health products stores, clinics, and centers for disease control (Fig. 4a), the second category of general hospitals and specialist hospitals (Fig. 4b), and the third category of emergency medical centers (Fig. 4c). The extracted information includes name

³ The RCP2.6 scenario represents the low greenhouse gas emissions and is the most optimistic scenario.

⁴ <http://ditu.amap.com/>

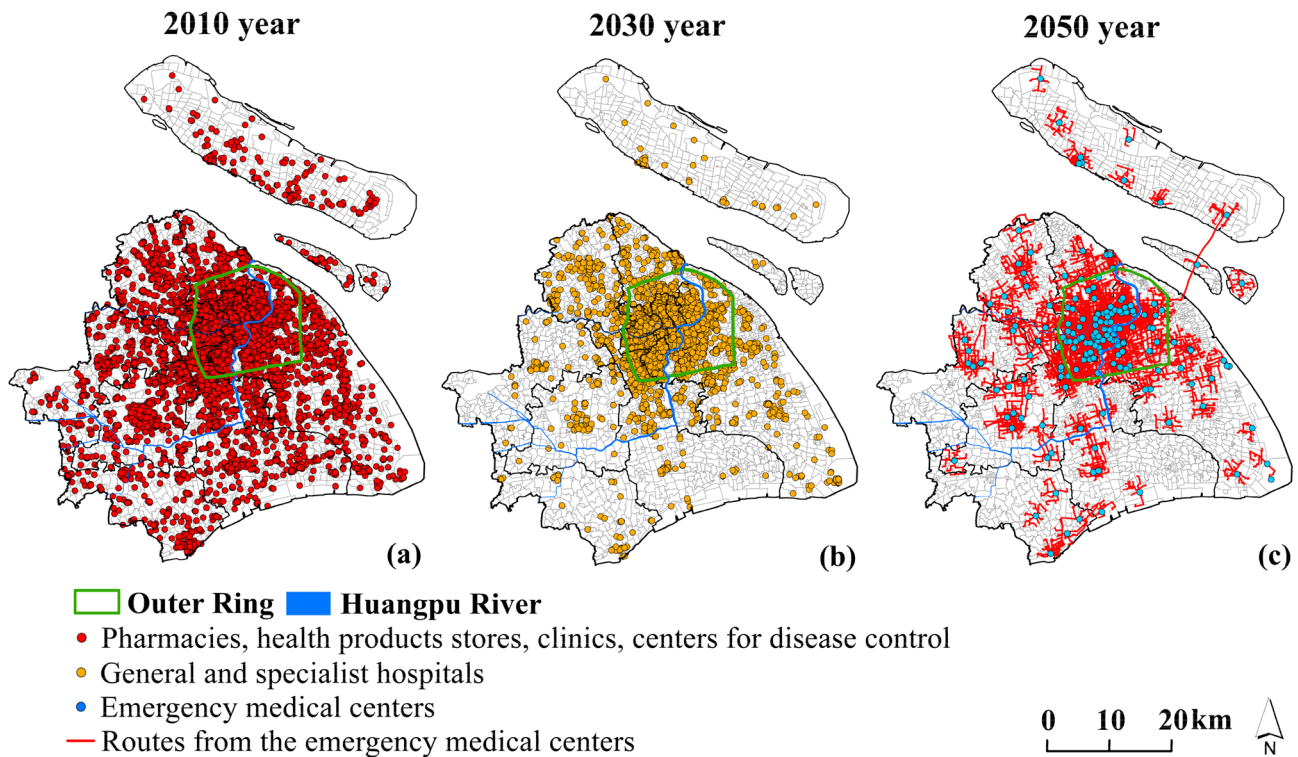


Fig. 4 Spatial distribution of two types of point of interest (POI) (a), (b) and emergency medical centers and total routes at the neighborhood committee level (c) in Shanghai

and coordinates. In particular, there were 199 emergency medical centers in the third category, which were used for accessibility analysis. The transportation network was obtained using a Python program to convert the transportation lines from AutoNavi open platform⁵ into a shapefile format, including 4320 access routes (Fig. 4c).

4 Results

This section presents the main results of this study, which include flood inundation maps; projected population and exposure to floods; the supply-demand ratio of medical resources; and the elderly's accessibility to emergency response services.

4.1 Flood Inundation Maps

Under the present conditions and the two future scenarios, the 1/100-year and 1/1,000-year flood inundation maps in 2010, 2030, and 2050 show the greatest risk of extreme floods for the southwest and northeast of Chongming Island,

the Qingpu and Songjiang low-lying areas in the west, and both banks of the Huangpu River.

Under the current situation (2010 year), the floodwall can withstand a 1/100-year flood, and the left bank of the middle reaches of the Huangpu River would be slightly submerged. For the 1/1000-year flood, the upstream area and right bank of the Huangpu River were seriously flooded, with additional failures scattered throughout the middle reaches (Fig. 5). If a 1/1000-year flood were to occur in year 2030 and 2050 under the RCP2.6 scenario, the floodwall in the upstream area of the Huangpu River could not withstand, while the downstream area is far safer.

However, under the RCP8.5 scenario, in the event of a 1/1000-year flood, the inundated area will be 2169 km², which is 135 km² larger than that under the RCP2.6 scenario. In particular, the downstream of the Huangpu River will be almost completely inundated. This is due to the lower level of protection in the upper reaches (protection level of 1 in 50 years). In the middle reaches of the Huangpu River, including the city center, structures such as large-scale high-rise buildings and underground space development engineering projects are causing land subsidence and deformation of the floodwall.

⁵ <https://lbs.amap.com/>

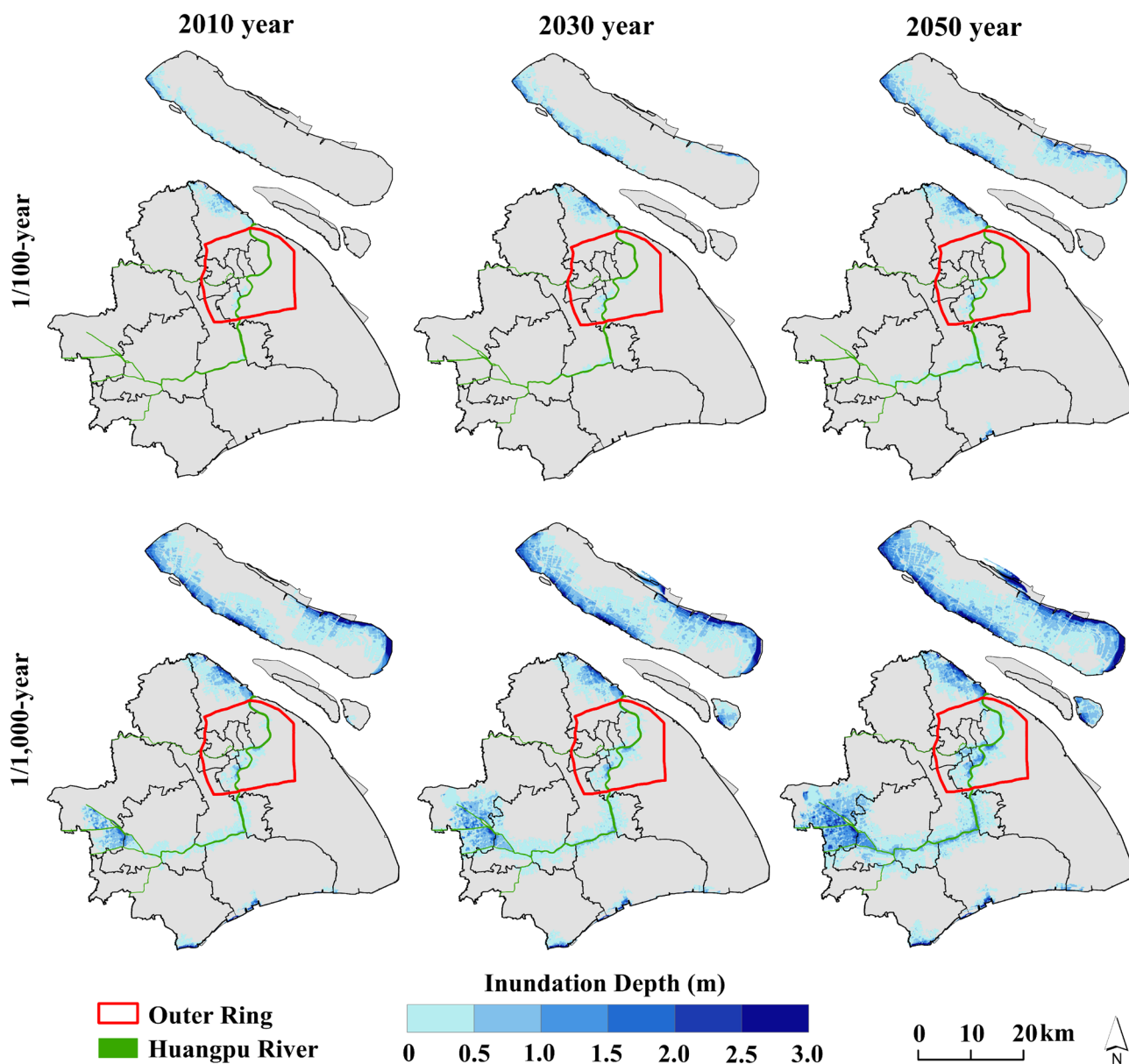


Fig. 5 Inundation maps of extreme floods at different return periods under the 2010 and RCP2.6 scenarios (years 2030 and 2050) in Shanghai

4.2 Projected Population and Exposure to Floods

The future population projection results show that Shanghai's population in 2030 and 2050 will be 31.46 million and 32.18 million, respectively, compared to 23.03 million in 2010. As time passes, the population of the central city and the three islands of Chongming gradually decreases, and the population of the suburbs gradually increases (Fig. 6).

The predicted numbers of Shanghai's elderly population under three situations (median estimate, lower bound at 5%, and upper bound at 95%) for 2030 and 2050 are shown in Fig. 7 and Table 1. We used the root mean square error (RMSE) to measure the average difference between

the predicted values and the true values. We calculated that the RMSE is 8.60, which means that the prediction error is small and can meet the research needs. We performed model fitting on the existing elderly population data from 1990 to 2019, and chose the coefficient of determination R -squared to characterize the fitting degree of the model, which can well reflect the accuracy of the prediction model. When the coefficient of determination R -squared is close to 1, it indicates that the model fitting effect is good. Finally, we used a quadratic polynomial model and obtained the coefficient of determination R -squared of 0.99, close to 1, which can well explain the variation of the dependent variable. We provide confidence intervals, with the lower and upper bounds

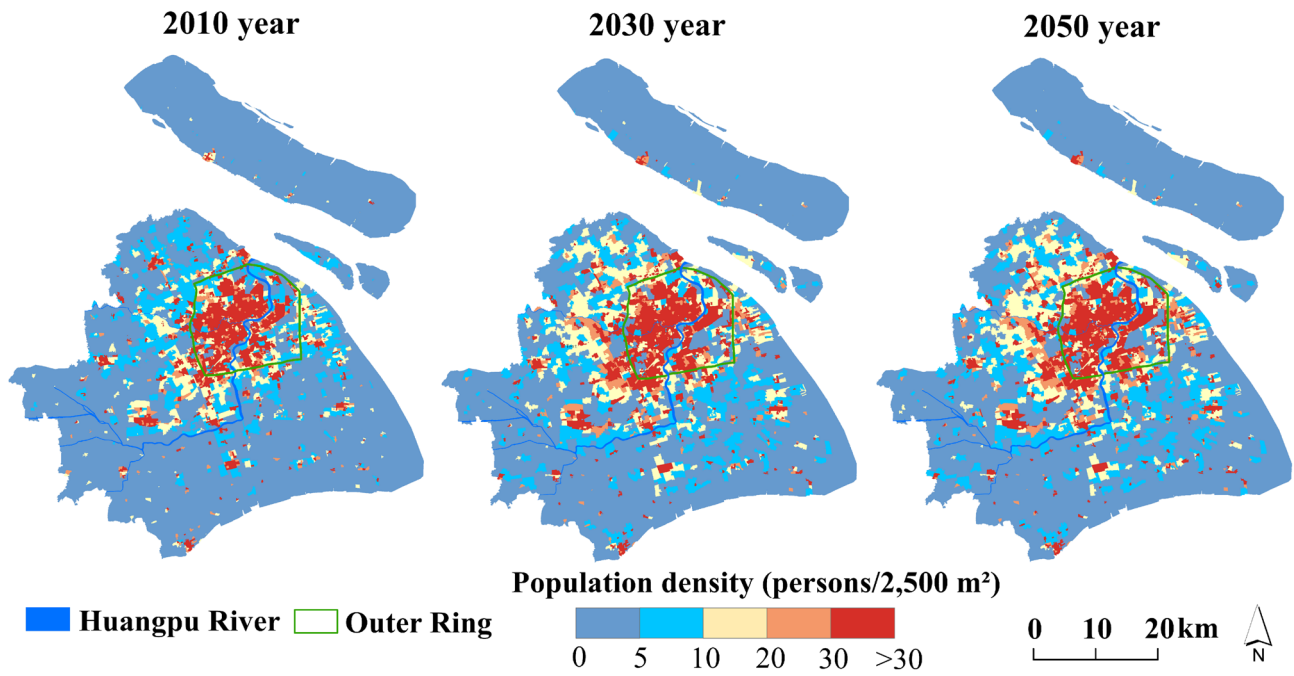


Fig. 6 Spatial distribution of population in Shanghai in 2010, and predictions for 2030 and 2050

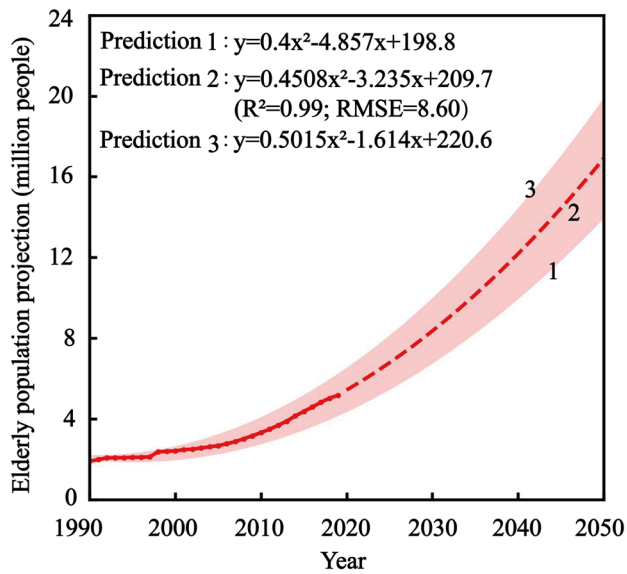


Fig. 7 Prediction of the elderly population in Shanghai. The dots indicate the actual elderly population per year; the dashed line indicates the projected elderly population per year (median values, prediction 2); and the shading indicates the 5% and 95% bounds (predictions 1 and 3).

indicating values corresponding to the 5th and 95th percentiles of the probability distribution, respectively.

Combined with the flood map, we obtained the spatial distribution of the affected total population and the elderly population exposed (Fig. 8). Under the RCP2.6

Table 1 Projected number of Shanghai’s elderly population (millions) in 2030 and 2050

	Elderly population in Shanghai	
	2030	2050
Prediction 1 (lower bound)	6.72	13.91
Prediction 2 (median estimate)	8.35	16.90
Prediction 3 (upper bound)	9.97	19.88

and RCP8.5 emission scenarios, the patterns of the three population exposure predictions are similar. The exposure of the elderly population in 2030 and 2050 is distributed along the Huangpu River, in the low-lying areas of the city center, and on Chongming Island, and the latter is the area with the highest exposure density of the elderly population (Fig. 8). Under the RCP2.6 scenario, the exposure proportion of the elderly population in 2030 will increase from 28.7 to 38.3% for a 1/100-year flood to 30.7 to 41.4% for a 1/1000-year flood under the three predictions of the elderly population. Except for the 1/100-year flood, under all other predictions in 2050, more than 50% of the elderly population will be exposed to the 1/100-year and 1/1000-year floods, and the highest exposure rate will be 69.1% (Table 2). Under the RCP8.5 scenario, the exposure rate of the elderly population can reach as high as 75.7% by 2050 (Table 3).

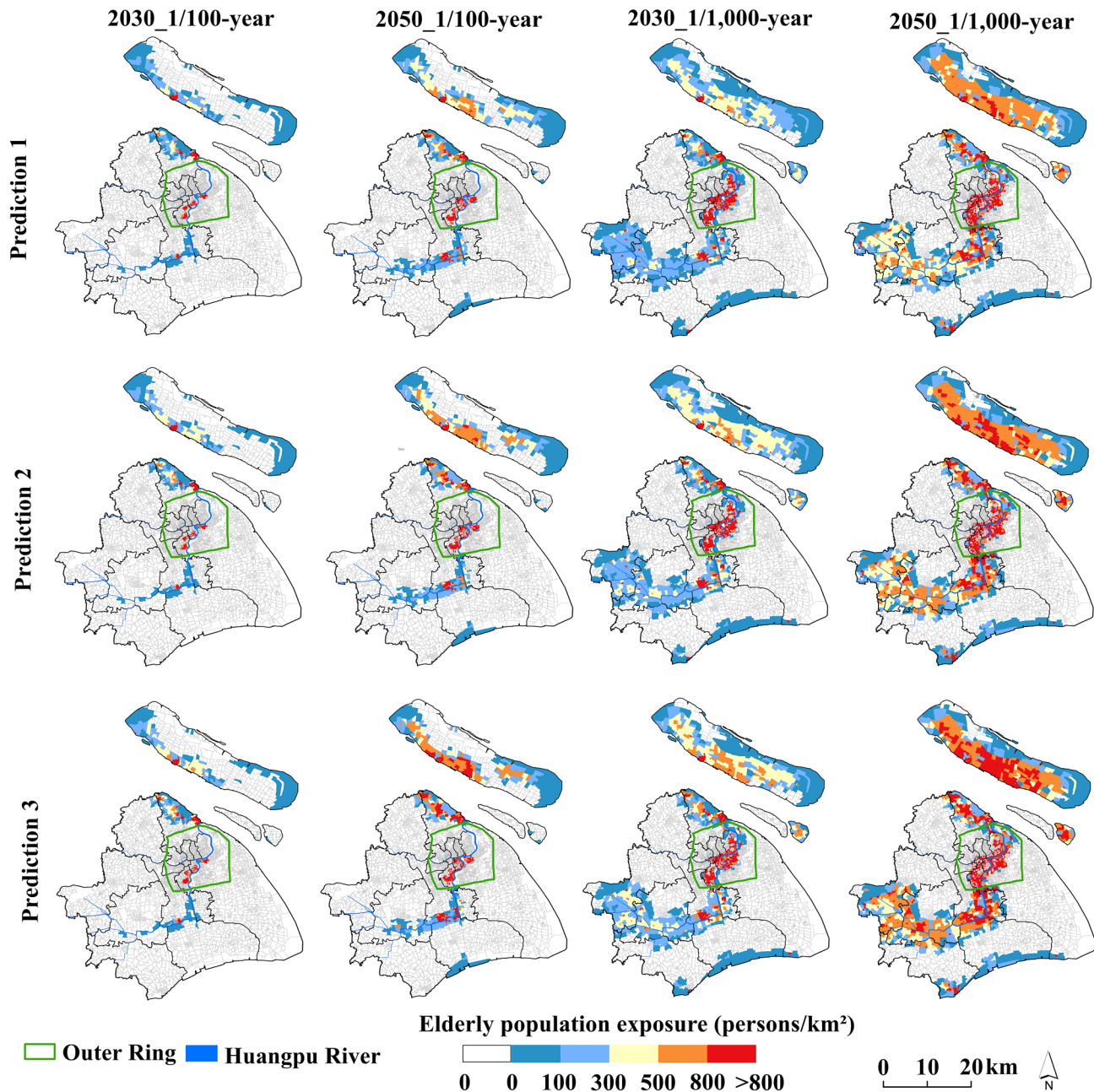


Fig. 8 Elderly population in Shanghai per unit area under the RCP2.6 scenario. *Prediction 1* lower bound, *prediction 2* median estimate, *prediction 3* upper bound. 2030_1/100-year means a 1/100-year flood in 2030, and so on.

4.3 Supply-Demand Ratio of Medical Resources

The spatial pattern of the supply-demand ratio shows that this ratio of the two types of POIs will be sufficient for the city center and the outer ring, except sporadic areas with extremely low supply-demand ratios that indicate a lack of medical resources (Fig. 9).

The medical resources on both sides of the Huangpu River will be severely scarce for 1/100-year and 1/1000-year

floods in 2030 and 2050, and these areas are also high exposure areas of the elderly population. In 2010, when a 1/100-year flood occurs, the supply-demand ratio of 15 or more is 32.7%, and the supply-demand ratio of 15 or more drops to 23.5% for a 1/1000-year flood. However, when the elderly population grows, according to prediction 2 (see Fig. 7), under the RCP2.6 and RCP8.5 scenarios, the supply-demand ratios of 15 or more will account for 9.5–10.0% of the total in 2030 and 3.0–3.2% in 2050 for a 1/1000-year flood.

Table 2 Exposure of the elderly population in Shanghai to extreme floods under the RCP2.6 scenario (persons)

	Year	Return period (years)	
		1/100 year	1/1000 year
Prediction 1 (lower bound)	2010	159,000 (21.9%)	720,000 (27.6%)
	2030	388,000 (28.7%)	1,600,000 (30.7%)
	2050	964,000 (42.5%)	3,974,000 (51.7%)
Prediction 2 (median estimate)	2030	452,000 (33.4%)	1,874,000 (35.9%)
	2050	1,171,000 (51.6%)	4,722,000 (61.5%)
Prediction 3 (upper bound)	2030	518,000 (38.3%)	2,158,000 (41.4%)
	2050	1,414,000 (62.4%)	5,310,000 (69.1%)

Percentage = (The elderly population exposed/Total exposed population) × 100%.

Table 3 Exposure of the elderly population in Shanghai to extreme floods under the RCP8.5 scenario (persons)

	Year	Return period (years)	
		1/100 year	1/1000 year
Prediction 1 (lower bound)	2010	159,000 (21.9%)	720,000 (27.6%)
	2030	442,000 (31.1%)	1,759,000 (33.5%)
	2050	1,212,000 (45.5%)	4,670,000 (55.7%)
Prediction 2 (median estimate)	2030	542,000 (38.1%)	2,122,000 (40.4%)
	2050	1,472,000 (55.2%)	5,673,000 (67.7%)
Prediction 3 (upper bound)	2030	596,000 (41.9%)	2,392,000 (45.5%)
	2050	1,733,000 (65.0%)	6,342,000 (75.7%)

Percentage = (The elderly population exposed/Total exposed population) × 100%.

The supply-demand ratio of medical resources of less than 5 accounts for 71.5–82.3% of the total in 2030 and 84.4–85.3% in 2050 for a 1/1000-year flood under the RCP2.6 and RCP8.5 scenarios. The supply-demand ratio of 15 or more in 2030 and 2050 will account for 10.4–11.3% and 3.7–3.8% of the total for a 1/100-year flood, respectively. The supply-demand ratio of medical resources of less than 5 accounts for 63.2–64.4% in 2030 and 81.2–82.2% in 2050 for a 1/100-year flood under the RCP2.6 and RCP8.5 emission scenarios. The results show that in the future, as the return period of extreme floods increases and the elderly population grows, the supply of medical services will need to increase to maintain the supply-demand ratio (see Fig. 9). Under the two emission scenarios and three predictions of elderly population, as the years and return periods increase, the difference between the supply-demand ratios of future medical resources and the 2010 values will become larger. Especially in 2050, when there is a 1/1000-year flood, the supply-demand ratio of medical resources declines significantly from the 2010 level to 30.2–36.8 (Fig. 10).

4.4 Accessibility to the Emergency Response Services

Routes to emergency medical services (with submerged water depth less than 30 cm) under extreme flood scenarios in different years and return periods were used to compute

the accessibility of the flood-affected sites (neighborhood committees) by distance (Fig. 11). We divided the accessibility into 5 levels: 0–0.5, 0.5–1.0, 1.0–1.5, 1.5–2, > 2, which represent very low, low, medium, high, and extremely high accessibility. Areas with accessibility exceeding 1 account for 25.4% and 10.2%, respectively, for the 1/100-year and 1/1000-year return periods in 2010.

Under the RCP2.6 scenario, these numbers change to 8.4% for a 1/100-year flood and 3.6% for a 1/1000-year flood in 2030. Under the RCP8.5 scenario, the proportion of areas with accessibility exceeding 1 is 5.2% for a 1/100-year flood and 2.5% for a 1/1000-year flood in 2030. Under the RCP2.6 and RCP8.5 emission scenarios, the proportion of areas with accessibility exceeding 1 falls below 0.3% in 2050. For a 1/100-year flood, some parts of the road network along the Huangpu River and in Xuhui and Pudong New Area (Shanghai's city center waterfront along the Huangpu River) will be impassable, and individual emergency response centers will almost lose their emergency service function due to their location in the inundation area. For a 1/1000-year flood, the entire central urban area near the Huangpu River is affected by flooding, resulting in traffic interruptions. The number of hospitals located in the flooded area is also significantly higher than that in a 1/100-year flood event, which seriously affects the urban emergency medical service function on both sides of the Huangpu River. Under extreme flood scenarios, some

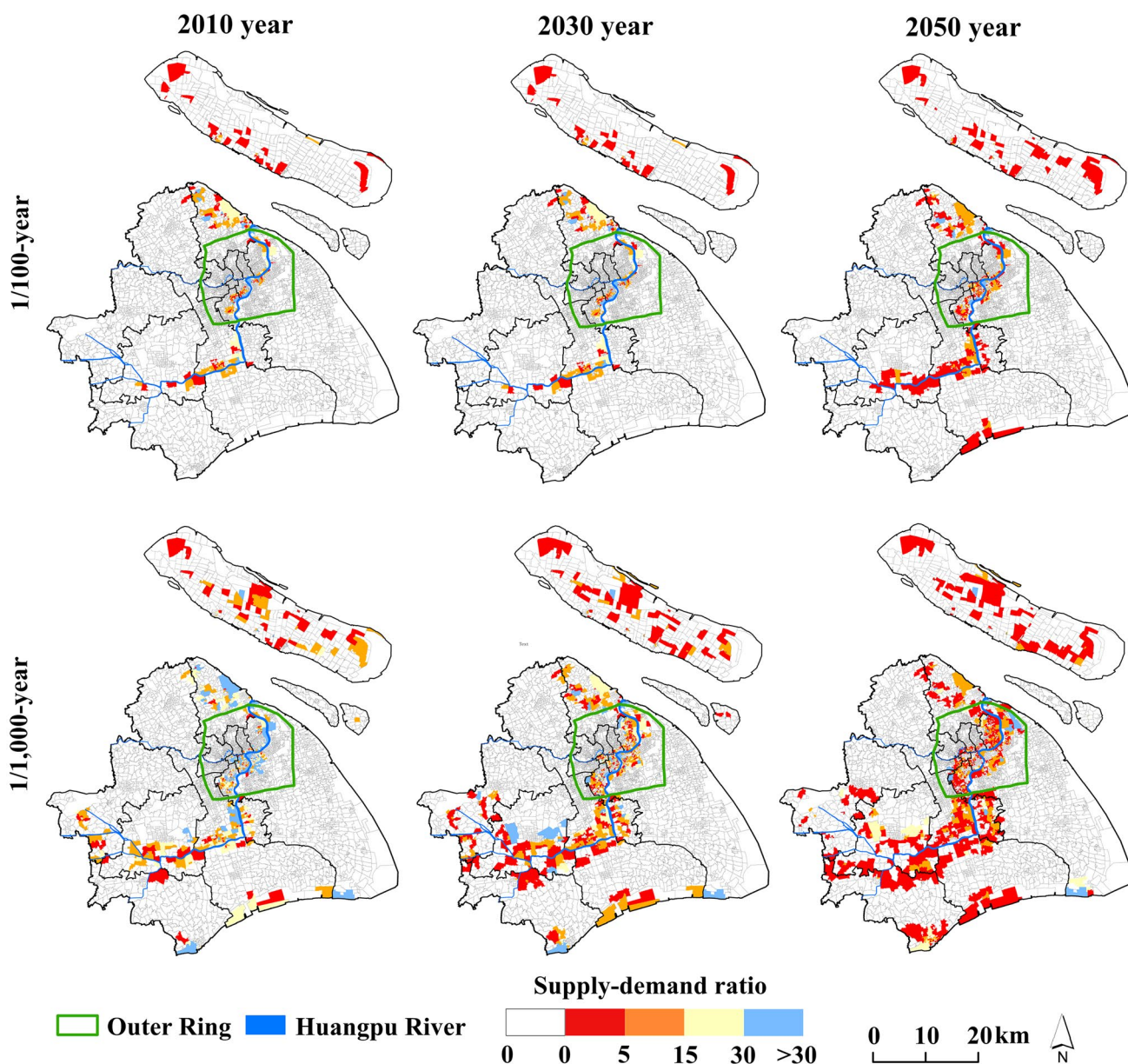


Fig. 9 Supply-demand ratio of the two types of point of interest (POI) for the elderly population in Shanghai in 2010, 2030, and 2050 for 1/100-year and 1/1000-year floods under the RCP2.6 scenario

social welfare agencies cannot reach emergency medical centers due to partial road blockage, and the emergency accessibility of some rescue points is insufficient. In addition, although the area affected by floods does not account for a high proportion of the total area of the central city, the places affected by floods are mainly concentrated in the important central business district, administrative district, and high-end residential areas on both sides of the Huangpu River, which are critical areas for urban public emergency services. Therefore, the impact of flood disasters on the overall level of urban public medical emergency services is still very significant.

5 Discussion

This section discusses the supply-demand of medical resources for the elderly in the future, several recommendations to improve emergency response services, and the limitations of this study.

5.1 Insufficient Medical Resources for the Elderly Population in the Future

Shanghai is a top financial center and has one of the best flood protection systems in China. The floodwalls

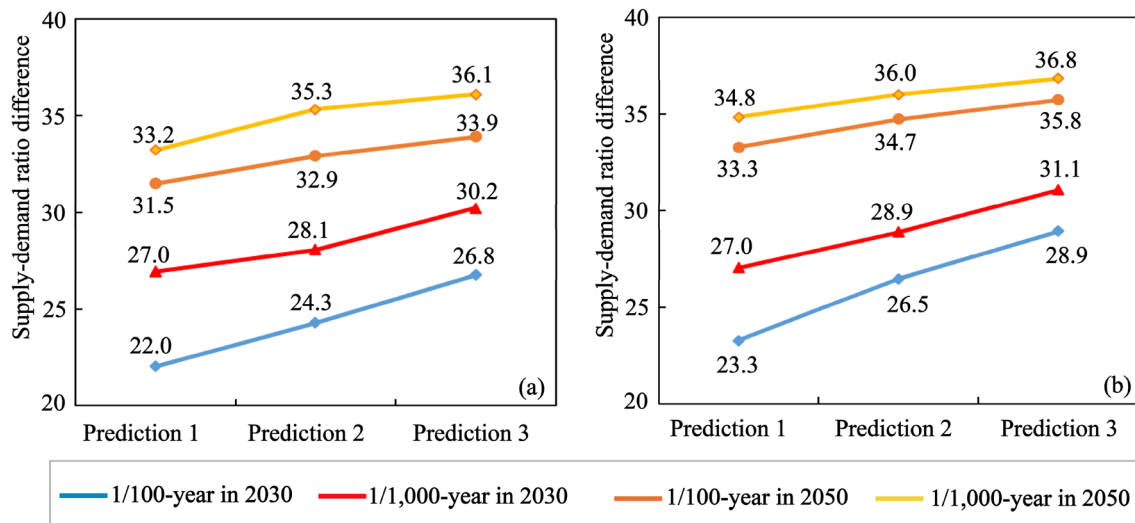


Fig. 10 Difference between the supply-demand ratio of the two types of point of interest (POI) in Shanghai in 2030/2050 and the 2010 values under the RCP2.6 scenario (a) and the RCP8.5 scenario (b)

along the Huangpu River are designed for a 1/1000 storm surge in the city center and against a 1/50-year flood in the upstream area (Wang et al. 2012). These engineering works were constructed following the devastating flooding in Shanghai that resulted from Typhoon Winnie in 1997. This study confirms the findings of Du et al. (2020) that in the future flood risk will face a significant increase.

As the years and return periods increase, especially in 2050, when a 1/1000-year flood occurs, the supply-demand ratio of medical resources declines significantly from the 2010 level. It shows that in the future extreme floods will have a strong impact on the supply-demand ratio of medical resources for Shanghai's elderly population. Although Shanghai has better medical resources compared to other cities in China, with the growth of the elderly population in the future, it is necessary for policymakers to consider increasing medical resources in areas with high elderly population exposure. Spatial distribution maps can provide clear information and references for decision makers to make robust decisions. In the 1/100-year and 1/1000 year flood scenarios in 2030 and 2050, in some parts of the low-lying city center and the areas on both sides of the Huangpu River, the supply and demand ratio of medical resources will be seriously low. These are also exposure areas for the elderly population. Therefore, the relevant government departments in Shanghai need to add medical services in specific neighborhood committees to meet the future medical resource needs of the elderly population in dealing with extreme floods, and to better respond to flood risks.

5.2 Improve Emergency Response Services

The results of this study show that as the return period increases, the flooded area continues to increase, the routes for emergency medical centers to reach the neighborhood committees decrease, and the area with accessibility exceeding 1 declines. Emergency responders should plan not only for the implementation of their current services, but also for more frequent floods in the future. Such plan adjustments might include using updated flood and traffic condition information to guide route selection when dispatching response vehicles.

Based on our findings, we also propose the following recommendations to the decision makers. First, in view of the significant impact of floods on the emergency response capabilities of urban public services, the urban emergency management departments need to adopt response measures to ensure the accessibility of key nodes and sections of the road network and emergency public services. Second, early warning systems and real-time flood forecasting may provide timely information for emergency responders. Finally, a real-time route navigation option could allow vehicles to safely pass (or avoid) flooded areas, ensuring spatial accessibility of urban emergency public services.

5.3 Other Response and Adaptation Measures and Limitations of this Research

It is necessary to increase other rescue equipment (for example, helicopters) for urban emergency rescue to improve rescue capabilities (Shi et al. 2020; Li et al. 2021). The

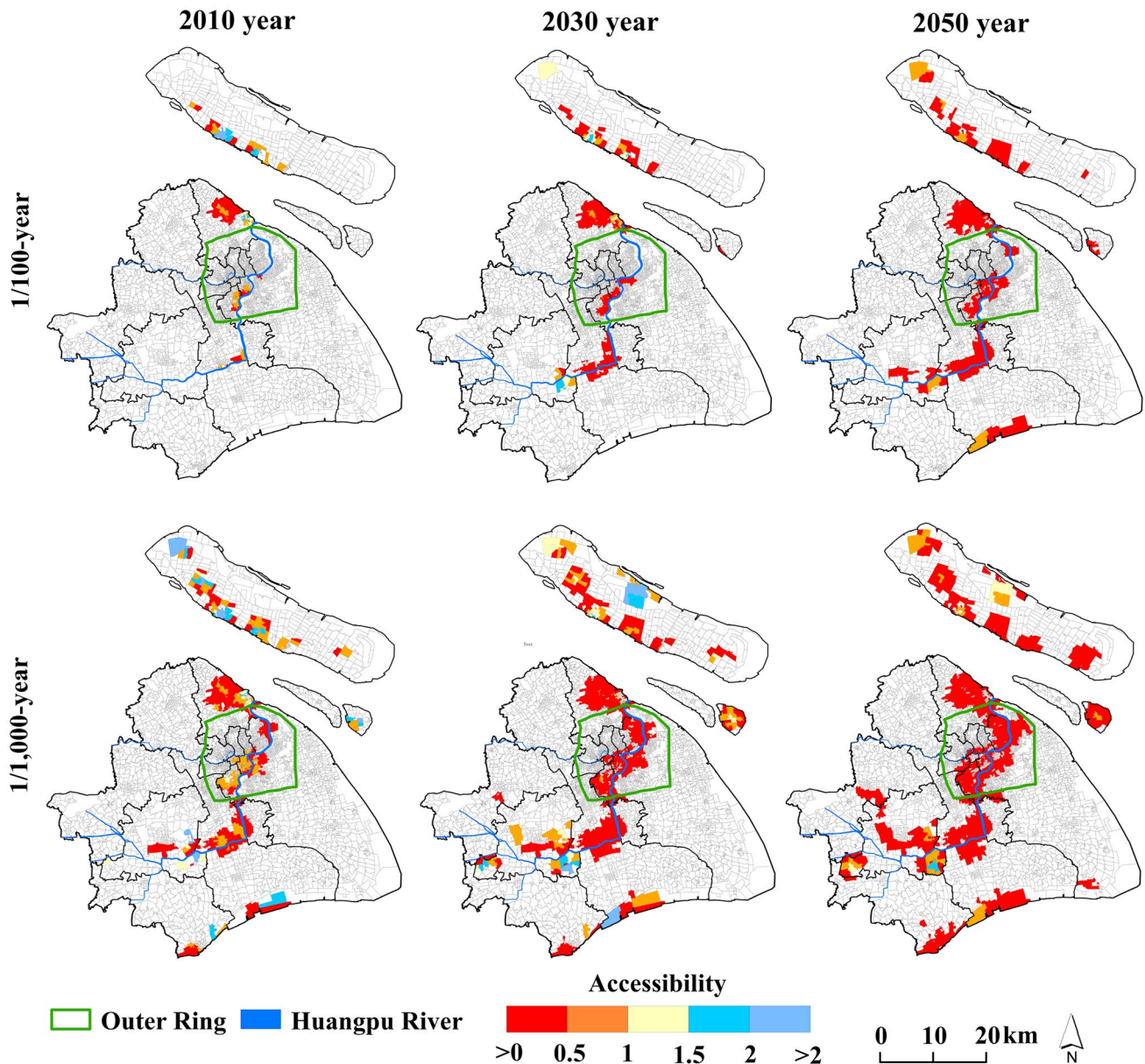


Fig. 11 Accessibility to the emergency medical centers of the neighborhood committees in Shanghai under the RCP2.6 scenario

municipal and local governments should attach great importance to disseminating disaster prevention knowledge to the communities, strengthen the effective integration of elderly care and disaster prevention policies, as well as to developing community flood early warning systems and disaster management training courses (Liang et al. 2017).

There are also some limitations to our study. First, we did not characterize the dependence between flood drivers for this location. In the future, we need to capture the multivariate joint distribution of flood drivers (Couason et al. 2022; Wang et al. 2023). Second, there are uncertainties in vehicle speed changes due to flooding and changes in real-time traffic flow distribution on the road network. In future

research, urban traffic big data (for example, taxi trajectory data) should be introduced to provide more realistic spatiotemporal observation and simulation data for urban road network traffic (vehicle speed).

5.4 Generalization of the Approach

The proposed framework can be generalized and applied to other areas for the accessibility analysis of the elderly population to the healthcare services during coastal floods. To apply the population projection module, flood scenario analysis module, and supply-demand and accessibility module to other cities, the following data are needed:

- 1) Time series data of total and elderly populations, ideally at the resolution of district, subdistrict/township, or the smallest administrative unit; the duration should be several decades, and the variables should include age, fertility, mortality, life expectancy, sex ratio at birth, and constraints such as the capacity to accommodate the population, population-related governmental policies, and migration.
- 2) Digital elevation data.
- 3) Station-based tide levels in the last decade, sea level rise, land subsidence data, and floodplain topography.
- 4) POIs data of medically-relevant locations.

6 Conclusion

This study used a combination of exposure analysis, supply-demand ratio analysis, and emergency response analysis to evaluate the current and future (2030 and 2050) exposed elderly population, medical resources, and accessibility of emergency services when impacted by predicted extreme floods with various return periods to identify potential threats for the elderly population in the future. The main conclusions are:

- 1) Under the RCP2.6 and RCP8.5 emission scenarios, the spatial patterns of predicted population exposure are similar. Exposure will be the highest along the Huangpu River, in the low-lying areas of the city center, and on Chongming Island in Shanghai.
- 2) As the years and return periods increase, the difference between the supply and demand ratios of medical resources in the future and that in 2010 becomes larger, indicating that extreme floods will have major impacts on the supply-demand ratio of medical resources for Shanghai's elderly population, assuming no adaptation to the new reality of demography and flood hazard.
- 3) With the future growth of the elderly population, the accessibility of emergency services will decrease, and most neighborhood committees will have poor accessibility to emergency response centers in the city of Shanghai.

The results of this study provide some references for policymakers in Shanghai, and the proposed framework can be applied to other areas for evaluating the accessibility of the elderly population to medical services during future extreme floods.

Acknowledgments This research was funded by the National Natural Science Foundation of China (Grant Nos. 41971199, 42371088, 42171080), and the National Social Science Foundation of China (Grant No. 18ZDA105). Xinmeng Shan is thankful for the financial support from the program of China Scholarships Council (Grant No.

202206140063), and the East China Normal University Academic Innovation Promotion Program for Excellent Doctoral Students (Grant No. YBNLTS2023-003).

Open Access This article is licensed under a Creative Commons Attribution 4.0 International License, which permits use, sharing, adaptation, distribution and reproduction in any medium or format, as long as you give appropriate credit to the original author(s) and the source, provide a link to the Creative Commons licence, and indicate if changes were made. The images or other third party material in this article are included in the article's Creative Commons licence, unless indicated otherwise in a credit line to the material. If material is not included in the article's Creative Commons licence and your intended use is not permitted by statutory regulation or exceeds the permitted use, you will need to obtain permission directly from the copyright holder. To view a copy of this licence, visit <http://creativecommons.org/licenses/by/4.0/>.

References

- Arrighi, C., M. Pregolato, R.J. Dawson, and F. Castelli. 2019. Preparedness against mobility disruption by floods. *Science of the Total Environment* 654: 1010–1022.
- Bai, C., and X.Y. Lei. 2020. New trends in population aging and challenges for China's sustainable development. *China Economic Journal* 13(1): 3–23.
- Bukvic, A., J. Gohlke, A. Borate, and J. Suggs. 2018. Aging in flood-prone coastal areas: Discerning the health and well-being risk for older residents. *International Journal of Environmental Research and Public Health* 15(12): Article 2900.
- Chen, M.R., and S.P. Wang. 2000. Stormtide disaster and its forecast in Shanghai City. *Journal of Catastrophology* 15(3): 26–29.
- Cheng, X.T. 2020. Flood risk and flood management policies in China. In *Annual report on China's response to climate change*, ed. W. Wang, and Y. Liu, 49–65. Singapore: Springer.
- Chien, H.J., and Y.F. Chen. 2017. Rejuvenate Taiwan: Time to act now. Strategies of fewer children and population aging in Taiwan. *Journal of the Formos Medical Association* 116(3): 137–138.
- Coles, D., D.P. Yu, R.L. Wilby, D. Green, and Z. Herring. 2017. Beyond “flood hotspots”: Modeling emergency service accessibility during flooding in York, UK. *Journal of Hydrology* 546: 419–436.
- Couasnon, A., P. Scussolini, T.V.T. Tran, D. Eilander, S. Muis, J. Keesom, J. Dullaart, and Y. Xuan et al. 2022. A flood risk framework capturing the seasonality of and dependence between rainfall and sea levels: An application to Ho Chi Minh City Vietnam. *Water Resources Research* 58(2): Article 102037.
- Crimmins, A. 2016. *The impacts of climate change on human health in the United States: A scientific assessment*. Washington, DC: Global Change Government.
- Du, S.Q., P. Scussolini, P.J. Ward, M. Zhang, J.H. Wen, L.Y. Wang, E. Koks, and A. Diaz-Loaiza et al. 2020. Hard or soft flood adaptation? Advantages of a hybrid strategy for Shanghai. *Global Environmental Change* 61: Article 102037.
- Fang, J.Y., R.J. Nicholls, S. Brown, D. Lincke, J. Hinkel, A.T. Vafeidis, S.Q. Du, and Q. Zhao et al. 2022. Benefits of subsidence control for coastal flooding in China. *Nature Communications* 13(1): 1–9.
- Fang, J.Y., T. Wahl, Q. Zhang, S. Muis, P. Hu, J. Fang, S.Q. Du, and T.F. Dou et al. 2021. Extreme sea levels along coastal China: Uncertainties and implications. *Stochastic Environmental Research and Risk Assessment* 35(2): 405–418.

- Gallagher, J., and D. Hartley. 2017. Household finance after a natural disaster: The case of Hurricane Katrina. *American Economic Journal: Economic Policy* 9(3): 199–228.
- Gill, I.S., M. Raiser, A. Dallólio, T. Packard, and J. Zalduendo. 2012. *Golden growth: Restoring the Lustre of the European Economic Model*. Washington, DC: World Bank.
- Green, D., D.P. Yu, I. Pattison, R. Wilby, L. Boshier, R. Patel, P. Thompson, and K. Trowell et al. 2017. City-scale accessibility of emergency responders operating during flood events. *Natural Hazards and Earth System Sciences* 17(1): 1–16.
- Gu, H.H., Q.S. Du, B.G. Liao, J.H. Wen, C.X. Wang, R.S. Chen, and B. Chen. 2018. A hierarchical pattern of urban social vulnerability in Shanghai, China and its implications for risk management. *Sustainable Cities and Society* 41: 170–179.
- Hausfather, Z., and G.P. Peters. 2020. Emissions – The “business as usual” story is misleading. *Nature* 577(7792): 618–620.
- Kan, W.S., and R.P. Lejano. 2023. Relationality: The role of connectedness in the social ecology of resilience. *International Journal of Environmental Research and Public Health* 20(5): Article 3865.
- Kiran, K.C., J. Corcoran, and P. Chhetri. 2020. Measuring the spatial accessibility to fire stations using enhanced floating catchment method. *Socio-Economic Planning Sciences* 69: Article 100673.
- Kirezci, E., I.R. Young, R. Ranasinghe, S. Muis, R.J. Nicholls, D. Lincke, and J. Hinkel. 2020. Projections of global-scale extreme sea levels and resulting episodic coastal flooding over the 21st Century. *Scientific Reports* 10(1): Article 11629.
- Kopp, R.E., R.M. Horton, C.M. Little, J.X. Mitrovica, M. Oppenheimer, D.J. Rasmussen, B.H. Strauss, and C. Tebaldi. 2014. Probabilistic 21st and 22nd century sea level projections at a global network of tide gauge sites. *Earth's Future* 2: 383–406.
- Kron, W. 2005. Flood risk = hazard • values • vulnerability. *Water International* 30(1): 58–68.
- Li, M.Y., M.P. Kwan, J. Chen, J. Wang, J. Yin, and D.P. Yu. 2021. Measuring emergency medical service (EMS) accessibility with the effect of city dynamics in a 100-year pluvial flood scenario. *Cities* 117: Article 103314.
- Li, M.Y., F.H. Wang, M.P. Kwan, J. Chen, and J. Wang. 2022. Equalizing the spatial accessibility of emergency medical services in Shanghai: A trade-off perspective. *Computers, Environment and Urban Systems* 92: Article 101745.
- Liang, P.J., W. Xu, Y.J. Ma, X.J. Zhao, and L.J. Qin. 2017. Increase of elderly population in the rainstorm hazard areas of China. *International Journal of Environmental Research & Public Health* 14(9): Article 963.
- Liu, K.L., Q.F. Li, and Z.H. Zhang. 2019. Distributionally robust optimization of an emergency medical service station location and sizing problem with joint chance constraints. *Transportation Research Part B: Methodological* 119: 79–101.
- Lome-Hurtado, A., P.C. White, and J.M. Touza. 2021. Impact of natural hazards on morbidity and physical incapacity of vulnerable groups in Mexico. *International Journal of Disaster Risk Reduction* 63: Article 102417.
- NYC Oem (New York City Office of Emergency Management). 2014. *New York City Hazard Mitigation Plan*. New York: NYC Office of Emergency Management.
- Qiu, B.L., C.L. Xu, Y. Liu, and T.T. Xu. 2014. Vulnerability assessment of the impact of sea level rise and storm surges on Shanghai. *Resources and Environment in the Yangtze Basin* 23(1): 149–158.
- Rizeei, H.M., B. Pradhan, and M.A. Saharkhiz. 2019. Allocation of emergency response centers in response to pluvial flooding-prone demand points using integrated multiple layer perceptron and maximum coverage location problem models. *International Journal of Disaster Risk Reduction* 38: Article 101205.
- Sawangnate, C., B. Chaisri, and S. Kittipongvises. 2022. Flood hazard mapping and flood preparedness literacy of the elderly population residing in Bangkok. *Thailand. Water* 14(8): Article 1268.
- Shi, Y., J.H. Wen, J.C. Xi, H. Xu, X.M. Shan, and Q. Yao. 2020. A study on spatial accessibility of the urban tourism attraction emergency response under the flood disaster scenario. *Complexity* 1–9: Article 9031751.
- Song, J., X.Y. Tian, J.Y. Yu, and G.Y. Li. 1981. *Population forecasting and population control*. Beijing: Beijing People's Publishing House.
- Tang, J., W.J. Li, J.Y. Fang, Z.H. Zhang, S.Q. Du, Y.J. Wu, and J.H. Wen. 2021. Scenario-based economic and societal risk assessment of storm flooding in Shanghai. *International Journal of Climate Change Strategies and Management* 13(4–5): 529–546.
- Tellman, B., J.A. Sullivan, C. Kuhn, A.J. Kettner, C.S. Doyle, G.R. Brakenridge, T.A. Erickson, and D.A. Slayback. 2021. Satellite imaging reveals increased proportion of population exposed to floods. *Nature* 596(7870): 80–86.
- Wang, G.X. 2003. Population and development: A comparative study of Shanghai and Tokyo. *Fudan Journal (Social Sciences)* 6: 10–17.
- Wang, F.H. 2015. *Quantitative methods and socio-economic applications in GIS*, 2nd edn. Boca Raton, FL: CRC Press.
- Wang, C., and B. Yarnal. 2012. The vulnerability of the elderly to hurricane hazards in Sarasota. *Florida. Natural Hazards* 63(2): 349–373.
- Wang, J., W. Gao, S.Y. Xu, and L.Z. Yu. 2012. Evaluation of the combined risk of sea level rise, land subsidence, and storm surges on the coastal areas of Shanghai China. *Climatic Change* 115(3–4): 537–558.
- Wang, Y.M., X. Ji, and C.Y. Liu. 2014. Study on prediction of population change in Shanghai. *Shanghai Journal of Economics* 3: 89–98.
- Wang, H., Y.Q. Xuan, T.V.T. Tran, A. Couasnon, P. Scussolini, L.N. Luu, H.Q. Nguyen, and D.E. Reeve. 2023. Changes in seasonal compound floods in Vietnam revealed by a time-varying dependence structure of extreme rainfall and high surge. *Coastal Engineering* 183: Article 104330.
- Wang, J., S. Yi, M.Y. Li, L. Wang, and C.C. Song. 2018. Effects of sea level rise, land subsidence, bathymetric change and typhoon tracks on storm flooding in the coastal areas of Shanghai. *Science of the Total Environment* 621: 228–234.
- Wolff, C., T. Nikolettopoulos, J. Hinkel, and A.T. Vafeidis. 2020. Future urban development exacerbates coastal exposure in the Mediterranean. *Scientific Reports* 10(1): Article 14420.
- Xia, T.Q., X. Song, H.R. Zhang, X.Y. Song, H. Kanasugi, and R. Shibasaki. 2019. Measuring spatio-temporal accessibility to emergency medical services through big GPS data. *Health & Place* 56: 53–62.
- Xian, S., J. Yin, N. Lin, and M. Oppenheimer. 2018. Influence of risk factors and past events on flood resilience in coastal megacities: Comparative analysis of NYC and Shanghai. *Science of the Total Environment* 610: 1251–1261.
- Yang, J., and L. Mao. 2018. Understanding temporal change of spatial accessibility to healthcare: An analytic framework for location factor impacts. *Health & Place* 51: 118–124.
- Yang, Y.H., J. Yin, M.W. Ye, D.X. She, and J. Yu. 2020. Multi-coverage optimal location model for emergency medical service (EMS) facilities under various disaster scenarios: A case study of urban fluvial floods in the Minhang district of Shanghai, China. *Natural Hazards and Earth System Sciences* 20(1): 181–195.
- Yin, J., S. Jonkman, N. Lin, D.P. Yu, J.C.J.H. Aerts, R. Wilby, M. Pan, and E. Wood et al. 2020. Flood risks in sinking delta cities: Time for a reevaluation?. *Earth's Future* 8: Article e2020EF001614.

- Yin, J., N. Lin, and D.P. Yu. 2016. Coupled modeling of storm surge and coastal inundation: A case study in New York City during Hurricane Sandy. *Water Resources Research* 52(11): 8685–8699.
- Yin, J., D.P. Yu, and B.G. Liao. 2020. A city-scale assessment of emergency response accessibility to vulnerable populations and facilities under normal and pluvial flood conditions for Shanghai, China. *Environment and Planning B-Urban Analytics and City Science* 48(8): 2239–2253.
- Yin, Z.E., J. Yin, S.Y. Xu, and J.H. Wen. 2011. Community-based scenario modelling and disaster risk assessment of urban rainstorm waterlogging. *Acta Geographica Sinica* 21(2): 274–284.
- Yin, J., D.P. Yu, Z.E. Yin, J. Wang, and S.Y. Xu. 2013. Modelling the combined impacts of sea-level rise and land subsidence on storm tides induced flooding of the Huangpu River in Shanghai China. *Climatic Change* 119(3–4): 919–932.
- Yu, D.P., and T.J. Coulthard. 2015. Evaluating the importance of catchment hydrological parameters for urban surface water flood modelling using a simple hydro-inundation model. *Journal of Hydrology* 524: 385–400.
- Yu, D.P., J. Yin, R.L. Wilby, S.N. Lane, J.C.J.H. Aerts, N. Lin, M. Liu, and H.Y. Yuan et al. 2020. Disruption of emergency response to vulnerable populations during floods. *Nature Sustainability* 3(9): 728–736.
- Zoraster, R.M. 2010. Vulnerable populations: Hurricane Katrina as a case study. *Prehospital and Disaster Medicine* 25(1): 74–78.